Conference paper

OPTO-ELECTRONICS REVIEW 7(2), 63–74 (1999)

Metalorganic vapour phase epitaxy of GaN and lateral overgrowth♣

B. BEAUMONT and P. GIBART*

Centre de Recherches sur l'HétéroEpitaxie et ses Applications, CRHEA-CNRS
Sophia Antipolis, 06560-Valbonne, France

Nitride semiconductor alloys have merged as the most promising materials for short wavelengths light emitting diodes (LEDs) and laser diodes (LDs). The GaInN multiquantum wells (MQW) structure was used as the active part of LDs and has presently proven to work at room temperature in cw mode for 10,000 h. These achievements would not have been possible without the emergence of new approaches in heteroepitaxy of GaN leading to layers exhibiting lower dislocation densities than those grown using conventional heteroepitaxy. Metalorganic vapour phase epitaxy (MOVPE) has demonstrated its ability to fabricate structures for optoelectronics GaN based devices. Several nitrogen sources have been tested, but so far NH_3 remains the best nitrogen precursor despite the stringent requirement of high V/III ratio in the vapour phase.

With the epitaxial lateral overgrowth (ELOG), high quality GaN layers have been obtained. HVPE or MOVPE can apply either this ELOG technology, on sapphire or 6H-SiC substrates. The dislocation densities in the overgrowth region are orders of magnitude lower than in the standard heteroepitaxial GaN layers.

Keywords: GaN, lateral overgrowth, MOVPE

1. Introduction

More than a quarter century has elapsed since the first demonstration of stimulated emission in GaN under optical pumping [1]. Progress has been slowed because of intrinsic difficulties linked to the elaboration of GaN. First of all, non-intentionally doped GaN grown either in bulk or as an epitaxial layer exhibits a high residual n–doping. This was first believed to be due to native defects like nitrogen vacancies. Indeed, oxygen is the most likely a source of residual n–doping together with native defects like Ga_i or complexes involving nitrogen vacancies with hydrogen like V_N-H^{2+}. For almost two decades, p doping of GaN was not feasible. Since the ionisation energy of any acceptor species is of the order of 200 meV, the hole concentration at 300 K obtained by p doping is only one hundredth of the acceptor impurity concentration. Therefore, to produce p-type doping, the n-residual doping should be as low as achievable. Magnesium, one of the most widely used acceptor species introduces during growth Mg-H complexes that passivate the acceptors. This H passivation limits the electrical activity of Mg; therefore an activation process is required to get full electrical activity of the Mg atoms. This was achieved either through low energy electron beam irradiation treatment (LEEBI) [2–3] or thermal annealing [4]. These thermal processes result in the breaking the Mg-H bond. Afterwards, devices based on III–V nitrides were demonstrated, first LEDs, then LDs [5] and recently LDs working in cw at room temperature lasting for 10,000 hours [6].

In the early days of GaN, only HVPE was achievable and the nitrogen precursor was NH_3. With the development of highly efficient growth technologies like MBE or MOVPE, a new start of nitride material science and optoelectronics occurred. However, growth of epitaxial layers of GaN either by MOVPE or MBE is not straightforward.

* e-mail: pg@crhea.cnrs.fr

♣ The paper presented there appears in SPIE Proceedings Vol. 3725, pp. 2–9.

2. Metalorganic vapour phase epitaxy of GaN

At the first sight, nitrogen would be the most obvious precursor and, indeed, is the most commonly used in GSMBE. The high binding energy (9.5 eV) of the nitrogen bond requires energetic dissociative process to get atomic nitrogen. Besides, molecular nitrogen interacts poorly with the surfaces of nitrides; the dissociative chemisorption of N_2 is very ineffective. As a result, an activation of nitrogen (by plasma or ionisation assistance) or the use of ammonia is necessary for effective growth of nitrides by GSMBE and MOVPE. Presently, NH_3 is the most widely nitrogen precursor used for the growth of GaN in MOVPE. However the requirement of high temperature for the epitaxial growth requires a high NH_3 partial pressure to avoid nitrogen loss during the growth. Therefore a very high V/III ratio should be used in the vapour phae (~10^4–10^5). Other potential nitrogen sources than NH_3 have been considered, but neither other nitrogen precursor, nor "single source" adducts have produced high quality GaN yet.

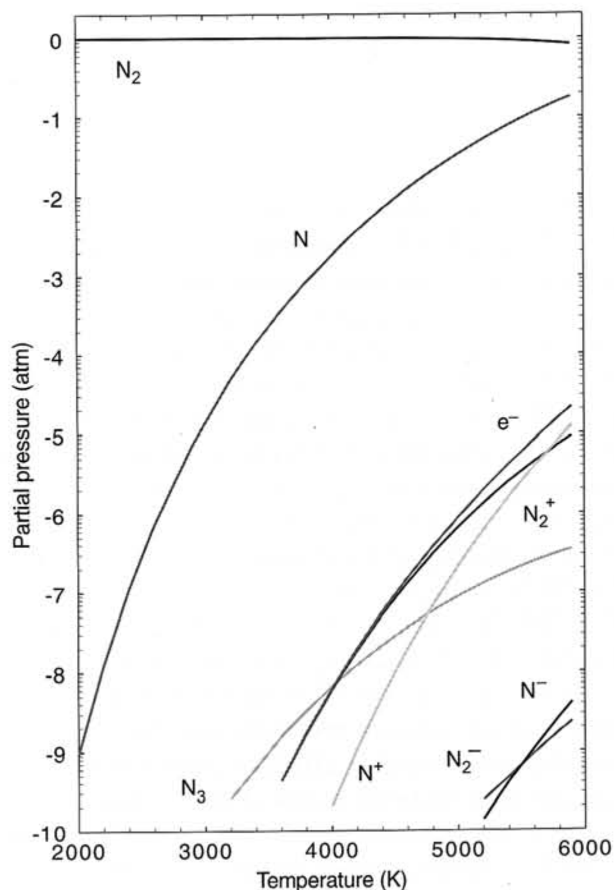

Fig. 1. Temperature dependence of nitrogen species equilibrium partial pressure for a starting pressure of N_2 of 10^5 Pa.

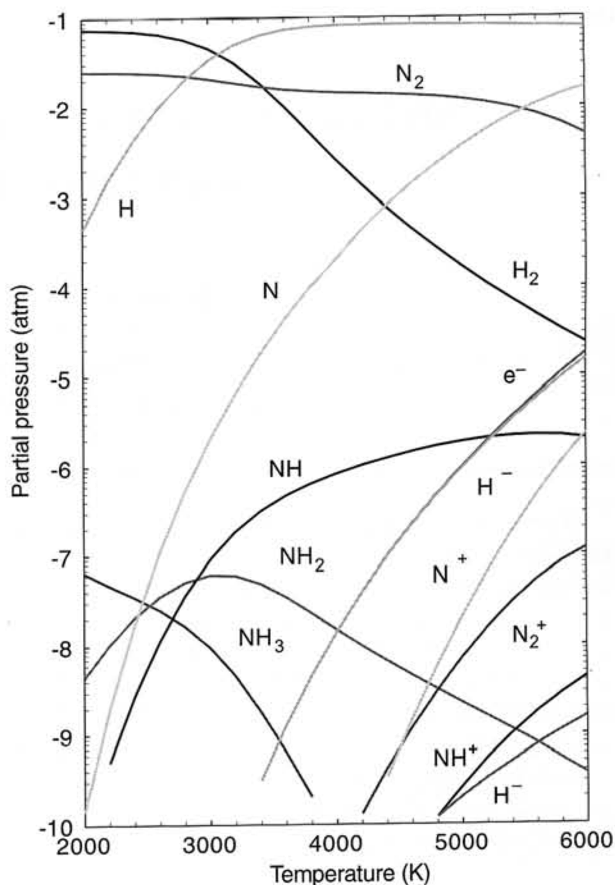

Fig. 2. Temperature dependence of equilibrium partial pressures of the species arising from the decomposition of NH_3, starting conditions $P_{NH_3} = 10^5$ Pa.

3. Rationale

The MOVPE process involves simultaneous heat, mass and momentum transport together with gas-phase and surface reactions. A full understanding of MOVPE process requires simultaneous resolution of the Navier-Stokes equation (fluid dynamics) together with thermodynamics and kinetics of the gas phase and also surface reactions. Models have been developed in which all these parameters are taken into account. At the stage of the choice of a nitrogen precursor, a thermodynamic evaluation has to be developed, although reaction pathways should be analysed in a further step. In a first approach, we have carried out straightforward calculations based upon the minimisation of free enthalpy of multicomponent systems. For these calculations, the GEMINI code was used and the thermodynamics data were provided by THERMODATA [7–9]. The lifetime of atomic nitrogens in MBE is so long that all of them are supplied to the growing interface. At low pressure ~10–100 Pa, where plasma assisted MOVPE takes place, the life-

 © 1999 COSiW SEP, Warsaw

time is still high enough whereas in atmospheric pressure MOVPE, the active radical formed are not the dominant source of nitrogen. N is supplied to the growing interface by heterogeneous decomposition of NH_3 [10].

3.1. Activation process of nitrogen

Significant amount of atomic nitrogen can be produced in plasma. Figures 1 and 2 show the calculated partial pressure of the atomic and molecular species resulting from the thermal decomposition of nitrogen in the temperature range 2000–6000 K. At very high temperatures, in the range of plasma temperatures, a significant amount of atomic nitrogen is formed. The photoluminescence spectrum (Fig. 3) is dominated by donor-acceptors pairs, the quality of the GaN layers obtained from a plasma source is too poor for practical use in devices.

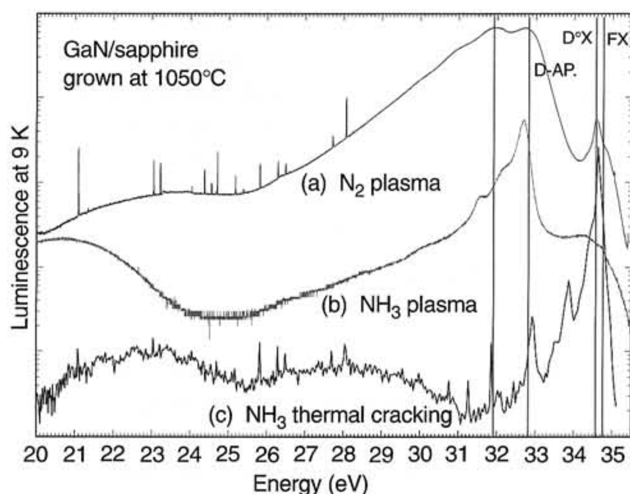

Fig. 3. Comparison between luminescence spectrum of GaN samples grown in similar conditions except the nitrogen precursor.

3.2. NH_3 as a precursor

Almost all present MOVPE reactors use NH_3 as a nitrogen source and high quality GaN has been produced. However, very high NH_3 over $Ga(CH_3)_3$ (TMG) partial pressure ratios are required to achieve the deposition of GaN. High purity NH_3 should be used to avoid impurities introduction. Not any reactive species like N, NH, NH_2 are produced in the thermal decomposition process. Kinetics barrier prevents NH_3 to be fully decomposed when reaching the growing interface. Most likely, the active species impinging the hot substrate is NH_3 and atomic Ga. It is established from GSMBE results that the sticking coefficient of NH_3 on GaN at about 1100 K is very low, (~10^{-2}). Even though NH_3 has proven its ability to produce high quality GaN, parasitic adduct formation between TMG and NH_3 occurs. To avoid premature mixing between TMG and NH_3, the growth chamber should be specially designed. At the growing interface, the decomposition of NH_3 produces atomic hydrogen, which is to some extending incorporated into the GaN layer.

This may cause passivation of an acceptor and post-growth annealing is required to destroy hydrogen-Mg complexes.

3.3. Activation process of NH_3

3.3.1. Plasma assisted NH_3 and hot filament

Since NH_3 leads to high quality GaN layers, it was expected than plasma assisted (PA) NH_3 would produce active nitrogen species suitable for the MOVPE growth of GaN. A thermodynamic estimation (Fig. 2) shows that even though N is produced in PA conditions, almost the whole hydrogen appears as atomic hydrogen. Even at 1800 K, which corresponds to growth conditions using a hot tungsten filament [8], a significant amount of atomic nitrogen is produced whereas almost not any active nitrogen species appears in the gas phase. GaN was grown from a NH_3 plasma source and from NH_3 precracked on a tungsten filament (at about 1800 K). At the low temperature, photoluminescence spectra (Fig. 3) the near band gap transition are almost quenched. The cubic modification of GaN is dominating the PL spectrum of samples grown from PA-NH_3. Hence, plasma NH_3 source does not produce high quality GaN. Atomic nitrogen most likely plays a major role and stabilises the cubic form of GaN.

3.3.2. Laser assisted MOVPE

Ultraviolet photolytic decomposition of TMGa and NH_3 may overcome the drawbacks of using high growth temperatures and high partial pressure of NH_3. Photodissociation of the precursors using a 193 nm laser is believed to produce Ga-CH_3 and NH which thereby allow to grow GaN thin layer with fair crystal quality at temperatures as low as 550°C [11]. When microwave plasma activation of NH_3 is produced in addition to laser assisted MOVPE (at 193 nm), rather good GaN was obtained [12].

3.4. Potential nitrogen precursors

When reviewing the chemistry of potential nitrogen precursor, it appears that molecules like N_4, N_4H_2, N_6 are highly unstable and could not be used in MOVPE [8]. Other molecules have been tested like dimethylhydrazine [13] or HN_3 [14,15]. HN_3 dissociatively chemisorbs on GaAs to form NH radicals and N_2 [15].

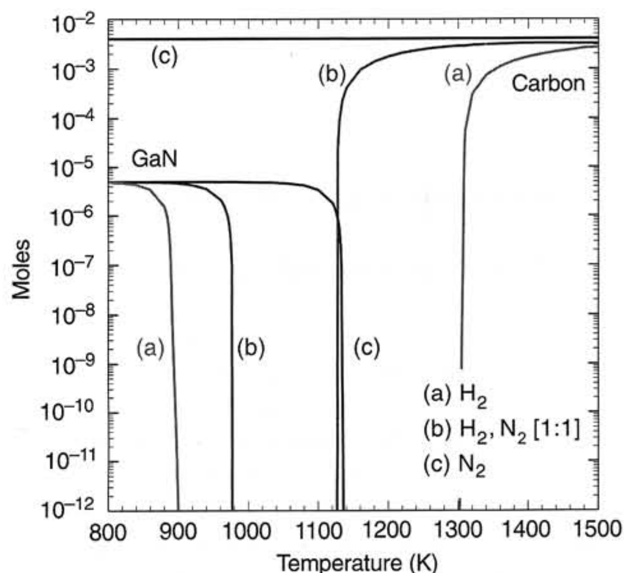

Fig. 4. Thermodynamic evaluation by minimisation of free enthalpy of the solid phase (GaN and carbon) for different composition of the carrier gas. Starting conditions, t-$BuNH_2$, 10^{-3} mole, $Ga(CH_3)_3$, 5×10^{-6} mole with (a) H_2, 1 mole; (b) H_2, 0.5 mole, N_2, 0.5 mole; (c) N_2, 1 mole. The calculations were carried out using the GEMINI code and thermodynamic data provided by THERMODATA, Grenoble.

On the other hand, molecules containing Ga-N bond like diethylgallium azide Et_2GaN_3 [16], dimethylazide [17] dimethylgallium azide Me_2GaN_3 [18], allow the deposition of GaN, but the quality of the layers is too poor and not all are suitable for optoelectronics.

It was expected that molecules like tert-butylamine (t-$BuNH_2$), which produce under thermal decomposition NH_2 and stable t-butyl radicals, would be suitable for GaN growth. This nitrogen precursor is liquid at room temperature and therefore can be used in MOVPE. Experiments have been carried out with this precursor as nitrogen source [7]. The growth process for the deposition of GaN from $Ga(CH_3)_3$ and t-$BuNH_2$ was basically similar to that of GaN from NH_3. A V/III ratio ranging from 100 to 200 was used (higher ratio would have required too high a t-$BuNH_2$ flow), and the carrier gas was either pure hydrogen, or pure nitrogen, or even a 1:1 mixture of H_2 and N_2. Whatever the growth conditions, composition of the carrier gas, V/III ratio, temperature, GaN was not deposited. Scanning electron analysis (in the EDX mode) reveals that the composition of the layer was mostly carbon. A thermodynamic analysis was carried out to try to explain these features even though it is well known that kinetics play also a determinant role.

Starting from the composition of the vapour phase used in the growth experiments, we evaluated the composition of the phases in equilibrium with the gas phase as a function of temperature by standard minimisation of the free enthalpy of the system. In Fig. 4 it is plotted the composition of the solid phase as a function of temperature for the same input parameters, t-butylamine, 10^{-3} mole, TMG, 5×10^{-6} mole, for three carrier gas compositions: (a) pure hydrogen (1 mole), (b) 0.5 mole N_2, 0.5 mole H_2, (c) pure nitrogen. According to these theoretical results, it appears that GaN cannot be grown above 900 K in pure H_2. Unfortunately, under pure nitrogen, carbon is the most likely solid to be deposited. On this thermodynamic basis, the observed results can be understood. This most likely rules out the use of this precursor for the GaN deposition.

3.5. Conclusions

Not any nitrogen organic precursor like triethylamine or t-butylamine is suitable for the deposition of GaN by MOVPE. Besides, plasma assisted growth, using N_2 or NH_3 did not produce high quality GaN. Presently, NH_3 seems to be the best nitrogen precursor for the MOVPE of GaN, despite intrinsic difficulties.

4. MOVPE of GaN from $Ga(CH_3)_3$ and NH_3

Sapphire is currently the most widely used substrate for the growth of GaN. However, the mismatch of about 14% and thermal expansion of about 80% between the sapphire (0001) basal plan and GaN requires a multi-steps growth process. Therefore, to get high quality GaN and to reduce the density of dislocations, heat treatment of the substrate and a given growth process should be accomplished. Before any deposition, pre-treatment under NH_3 is a key step to obtain high quality GaN. The so-called nitridation step is widely documented and will not be exhaustively discussed. Basically, nitridation is carried out at

 © 1999 COSiW SEP, Warsaw

1050°C under NH_3, this forms an amorphous AlON layer [19]. By HRTEM, it is evidenced than several AlN monolayers are formed on the top of the sapphire [20]. Also the duration of nitridation is of critical importance for the qualities of the GaN layers [21,22]. The structural and morphological quality of GaN grown by MOVPE on sapphire substrates is greatly enhanced by the use of the three-step growth.

4.1. Three-step growth

After nitridation

(i) in the initial growth step, a GaN or AlN buffer layer is deposited at a temperature of the order of 450–600°C (GaN grown directly on the sapphire results in nucleation of isolated islands), after the nucleation layer deposition,

(ii) the temperature is raised up to the growth temperature (1000–1100°C),

(iii) then, the growth of GaN is allowed to proceed.

The role of the low temperature (LT) nucleation layer is to promote uniform coverage on a sapphire. At LT the supersaturation is high, giving rise to high nucleation rates. Furthermore, the decreased mobility of surface species at LT promotes a uniform dispersion of nuclei that can effectively cover the substrate. The as grown nucleation layer consist of faceted (~ 20 nm high and wide) islands of highly faulted cubic GaN. This nucleation layer retains its coarse morphology and predominant cubic character upon heating at 1080°C, although the near surface region partially converts to hexagonal GaN. This process produces the films with densities of threading dislocations of 5×10^8 cm^{-3}, good mobility and optical properties [23–25].

The epitaxial relationships of GaN on sapphire are respectively (0001)GaN // (0001)sapphire; (01-10) GaN // (-2110)sapphire.

4.2. Optoelectronic properties

When optimising the growth process of GaN (i.e., duration of the nitridation at 1050°C, deposition temperature of the buffer layer, heat treatment of the buffer layer, deposition temperature, ratio V/III in the vapour phase), high quality GaN is obtained with RT mobility's up to 500–700 cm^2/Vs, residual carrier concentration 5×10^{16} cm^{-3}. However, to achieve these qualities, a proper real time *in situ* monitoring is required. The low temperature PL spectra are dominated by excitonic transitions (Fig. 3). Despite its present high cost, 6H-SiC has also proven to be a suitable substrate for the growth of GaN. When using 6H-SiC, an AlN buffer layer is first deposited at high temperature (HT) before the growth of GaN. The defect densities are somewhat lower than in GaN/sapphire.

4.3. Real time *in situ* monitoring by laser reflectometry

Since, like in most heteroepitaxial systems, the buffer layer is of critical importance; an *in situ* control of the growth process is required. Laser reflectometry (LR) was implemented to get an *in situ* tool for real-time diagnosis of the growth process [7–8]. LR primarily analyses the bulk epitaxial layer, the information provided by LR is straightforward. During growth of an epitaxial layer with a refractive index different from the substrate, the reflected light intensity follows a periodic function, the period of which is given by

$$\tau = \frac{\lambda \times \cos(\theta)}{2nV} \tag{1}$$

where λ is the wavelength of the laser, n is the refractive index of the layer at the growth temperature, V is the growth rate and Θ the angle of incidence. When the light is absorbed (optical absorption by the bulk layer) or scattered by roughening of the surface, the oscillations are damped by a factor α. The experimental set up involves a laser source at 632.8 nm (He-Ne laser) mechanically modulated and a detection system with a synchronous demodulator. Since nitrides are transparent at 632.8 nm, any damping would result from surface roughening. A typical recording of the reflectivity signal during an epitaxial growth of GaN on sapphire is given in Fig. 5.

Standard experiments start with a heat treatment of the sapphire under NH_3; on the reflectivity recording (Fig. 5, step a). The temperature is decreased down to 600°C (b), a GaN nucleation layer is subsequently deposited at 600°C, and the reflectivity increases (c). The ratio of the reflectivity of the growing buffer layer to the bare sapphire substrate can be used to monitor its thickness. Afterwards, the deposition of GaN is stopped (d), and then this nucleation layer experienced a short annealing at the growth temperature, 1050°C (e). The epitaxial growth is then allowed to proceed. The reflectivity signal shows undamped oscillations (Fig. 5 step f) which a perfect periodicity of 2.9 mn (corresponding to a growth rate of 2.8 µm/h). Such reflectivity measurements give a real time control of the growth process. Should the nucleation layer be improperly deposited, then the reflectivity will decrease during the annealing period resulting afterwards in damped oscillations. In

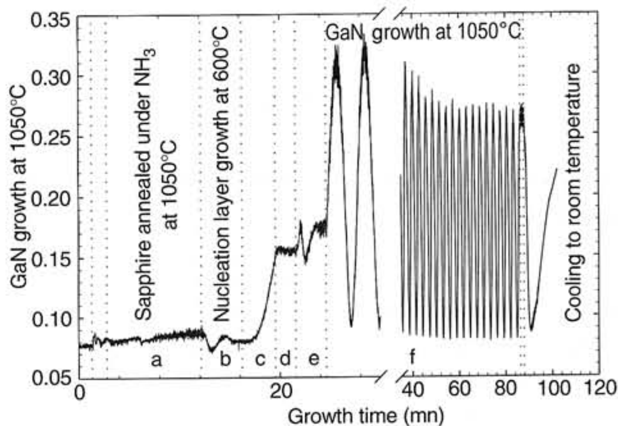

Fig. 5: Reflectivity recorded during a standard growth of GaN on (0001) sapphire.

other words, LR gives pertinent informations about the quality of the epitaxial layer both at the nucleation stage and during HT growth.

4.4. Structural assessment

The optoelectronic properties as well as surface quality's of GaN were observed to depend on the growth temperature of the GaN or AlN buffer layer, the thickness of the low temperature buffer layer, and nitridation time of the sapphire substrate, respectively. The as grown GaN does not present a perfect crystallographic quality, the linewidth obtained in double X-ray diffraction is of the order of 300 arcsec, the microstructure consist of columns of about 5 μm wide slightly misoriented (tilted and twisted) [25]. However, device quality GaN are currently grown by MOVPE or MBE on (0001) sapphire or 6H-SiC.

The large lattice and thermal expansion mismatches result in threading dislocations parallel to **c**, with densities ranging from 10^8 to 10^{11} cm^{-2}. Basically these threading dislocations with Burgers vector **c**, <0001>; **a**, 1/3 < 11–20> and mix **a+c**, 1/3 < 11 – 23> cross the active region of devices. Interestingly, in spite of these huge dislocation densities, optoelectronic devices like LEDs and LDs have a remarkable lifetime. Hence, a basic question that arises; do all these dislocations (and extended defects) act as non-radiative recombination centres? Indeed, some do. It has been proven that reduction of dislocations significantly lengthens the lifetime of minority carriers.

To pave the way towards this goal, three approaches can be followed:

(i) use of high quality GaN single crystals for homoepitaxy,

(ii) find new substrates with better lattice matching to GaN than sapphire or 6H-SiC,

(iii) set up a process to substantially reduce the density of dislocations.

The ELOG represents a new outstanding process in heteroepitaxy and will be discussed thereafter.

5. Epitaxial lateral overgrowth of GaN

5.1. Introduction

Selective epitaxy has been developed for III–V semiconductors like GaAs, InP or Si [26]. More precisely, selective epitaxy allows an accurate control of the size and shape of the overgrowth and therefore leads to the fabrication of quantum structures (wire and dots). Selective epitaxy in heteroepitaxial systems like GaAs/Si [27] or InP/Si [28] has also been widely used to overcome the deleterious effect of the large lattice mismatch.

Selective epitaxy of GaN by both MOVPE and HVPE on patterned GaN on sapphire has been previously reported [29–41]. Selective epitaxy corresponds to spatially controlled growth of an epitaxial layer through openings in a masking material, which is typically a dielectric such as silicon oxide or nitride.

Growth anisotropy corresponds to the occurrence of different growth velocities on different crystallographic planes. This has been observed in HVPE since at least two decades. For instance in GaAs, there are two orders of magnitude difference between the growth rates of $\{111\}_{Ga}$ and $\{111\}_{As}$. These features are understood by analysing the orientation dependence of the growth rate associated with surface kinetics. Growth anisotropy in MOVPE occurs only when diffusing molecules encounter different surface orientation within their mean free path λ_s.

A major problem in selective epitaxy is the ability to provide real selectivity, with growth occurring only in the openings and without any deposits formed on the mask. This can be achieved when the supersaturation of the growth nutrients on the dielectric mask is sufficiently low to prevent any deposition whilst the nucleation barrier on the exposed substrate in the openings is low in comparison. Therefore, in VPE (MOVPE or HVPE), the non-occurrence of growth on the mask depends on the reaction parameters: temperature, pressure and mole fraction of active species.

5.2. Experimental

The growth of GaN is performed by MOVPE vertical reactor operating at atmospheric pressure. The carrier gas is either pure N_2 or a mixture of N_2:H_2

 © 1999 COSiW SEP, Warsaw

(cf. §6). NH_3 and the different organometallic species [TMG, $(MeCp)_2Mg$] and diluted silane are introduced into the growth chamber by dedicated lines. The reactor is equipped with a HeNe laser reflectometry set-up used to monitor *in situ* the growth process. In the case of GaN regrowth on patterned GaN layers, it has been used to assess the completeness of the coalescence.

After deposition of the GaN buffer layer at 600°C, a 2–3 µm thick GaN layer is grown at 1080°C as usual. The threading dislocations density determined by TEM observation is in the 10^8 defects/cm^2 range.

The dielectric film was silicon nitride deposited on the GaN MOVPE layer. To this end, after completion of the growth of GaN, diluted silane is introduced in the vapour phase together with NH_3, allowing the *in situ* deposition of a thin (3 nm) layer. The silicon nitride was patterned using standard photolithography technology, revealing the free surface of the underlying GaN. For realisation of GaN pseudo-substrates, a 10 µm period grating with 5 µm wide stripes aligned along $[10\text{-}10]_{GaN}$ covering the whole area of the 1" substrate was used.

The selectivity of the growth is obtained with a high H_2 partial pressure (0.3 atm) in the growth chamber. When pure N_2 is used as carrier, a high density of nuclei is observed openings, no parasitic nucleation occurs on the dielectric mask.

5.3. GaN regrowth

GaN regrowth conditions used here are exactly the same as those used for epitaxy on non masked substrates. The shape of undoped GaN ribs after a few minutes of growth on patterned substrates is schematically drawn in Fig. 6. The GaN stripes present a trapezoidal cross section with a top C facet and two slants oriented on the average along {11-22}. These slants are themselves facetted by {10-11} plane segments due to the high instability of the {11-22} growth plane. The slants form an angle θ of 58° with the basal C plane.

Longer growth duration led to straight stripes with triangular section with {1-101} facets. Further growth results in full coalescence, however with not a smooth surface (Fig. 7). Perfect coalescence leaving smooth surfaces could be achieved by inducing growth of {11-20} facets, which are slow growing planes. Changing the growth temperature or the ratio V/III in the vapour phase can do this [32,42]. Addition of Mg in the vapour phase changes the growth mode.

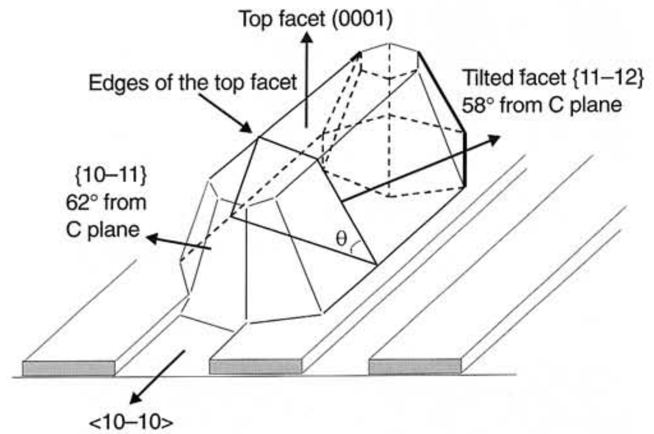

Fig. 6. Schematic view of the GaN stripes at the beginning of the regrowth on the patterned substrates of sapphire.

5.4. Regrowth of GaN with Mg doping

Particular growth conditions must be used to achieve favourable anisotropy of the growth, i.e., stable C facets and vanishing slants in order to obtain smooth and planar surface after coalescence is completed. Up to now, the growth temperature was the only parameter reported in the literature that can be adjusted to obtain flat coalesced samples [42]. The cross section of the GaN overgrown stripes tend to be delimited with increasing temperature by vertical sides and a stable C top facet. In a previous work, we reported that the anisotropy of GaN in standard growth conditions is dramatically modified by magnesium doping [43]. The main effect of Mg doping is to reduce to the growth rate in the [0001] direction without substantially modifying the growth rate of the slants. But the cross section of the GaN:Mg stripes is still delimited by facets having the same crystallographic orientation than in the undoped case.

Henceforth, keeping standard growth conditions, the anisotropy can be adjusted by introducing a given amount of Mg precursor in the vapour phase so that the slants become the fast planes and vanish further in. Fig. 8 shows the cross section of a sample obtained by lateral overgrowth of Mg-doped GaN on patterned GaN substrates (5 µm opening with 10 µm period). By contrast to Fig. 7, the surface of the overlayer is smooth and we can observe clearly the voids buried at the foot of coalescence boundaries. The planarisation was completed after about 2 hours of the growth run.

5.5. A two-step lateral overgrowth process

The most important feature expected from the lateral overgrowth process is a large reduction of the

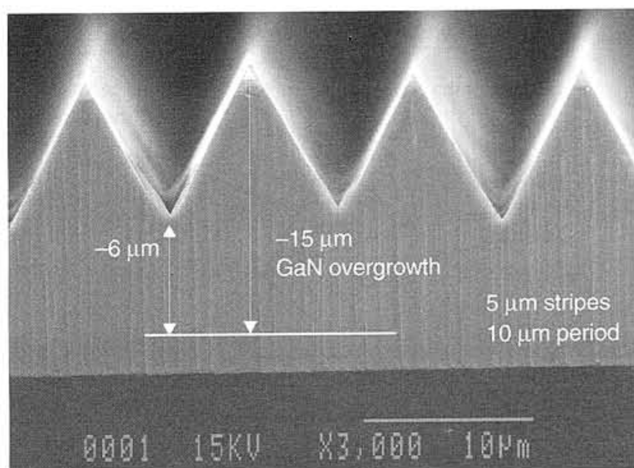

Fig. 7. SEM cross section of lateral overgrowth of undoped GaN in standard conditions. Though perfect coalescence is obtained (without voids at the coalescence boundaries due to very slow growth rates), no smoothing is achieved.

density of threading dislocations, which are mainly responsible for the short lifetime of high current injection devices or for the low mobility of undoped GaN. It is known that most of the threading defects are due to low angle boundaries existing within the mosaic structure of the epilayers. Moreover, these defects thread in the growth direction along the C axis and their density is not reduced substantially when increasing the thickness of the sample.

On one hand, we observed by HRTEM on cross sections of GaN samples grown on patterned substrates with anisotropy unfavourable to planarisation (i.e., no doping with standard growth conditions) that [39] the defect lines above the masked area lie parallel to the basal plane (0001) and the 90° line bending is initiated above the windows in the mask. This was also mentioned in the literature [44], where the bending points of the defect lines are reported to be contained in the trace of the {10-11} slants. On the other hand, when the growth anisotropy is favourable for the planarisation (high growth temperature or with Mg in the vapour phase), the overgrown GaN is reported to be free of emerging defects above the masked areas but the threading defects originated from the underlying GaN still propagate vertically through the mask opening and then emerge at the top surface of the overgrowth.

Therefore, a two-step process for the lateral overgrowth of GaN was implemented. In the first step, undoped GaN is overgrown until the top C facets vanish. In the second step, Mg is introduced to produce the coalescence with planarisation. The first step is intended to initiate defects lines bending over the openings of the mask, whereas the second step aims to planarisation.

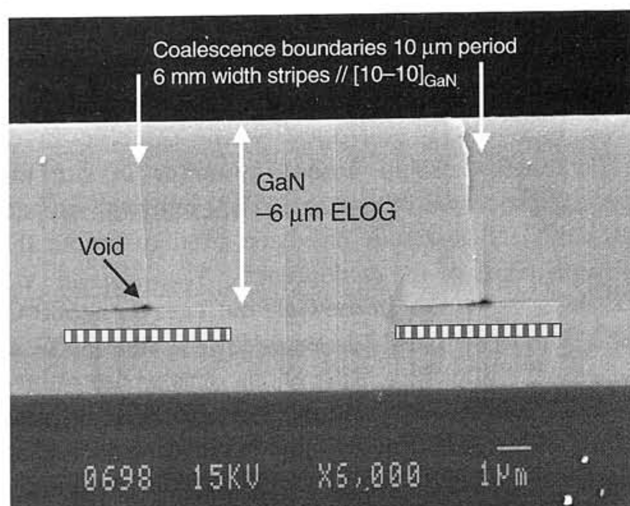

Fig. 8. SEM cross-section on Mg doped GaN overgrown on patterned substrate. Flat surface, contrasting with Fig. 6 is obtained due to the favorable growth anisotropy induced by the Mg doping. The mask appears as a very thin line above the dashed filled rectangle.

5.6. Structural assessment of the MOVPE GaN overgrowth

Figure 9 is the cross section TEM image of a two-step GaN overgrown on a patterned substrate. Threading dislocations present in the underlying masked GaN propagate vertically in the overgrown GaN through the mask opening. However, all of them bend by 90° at the points indicated by short arrows. During subsequent growth, the bent defect lines merge into the coalescence boundary. It is noticed that these points tend to organise along two lines visualised in the figure by the converging long arrows. A clear planar symmetry exists in this bending phenomenon. This reflects the symmetrical growth on both side of a plane parallel to and equidistant from the coalescence boundaries delimiting the periodic stripe patterns. The lines drawn through the bending points are likely to be the trajectory of the edges of the vanishing top C facets. This suggests that bending occurrs when a threading dislocation line crosses the right or left moving edge of the top C facet. As a result, when the top C facet has fully vanished at the end of step 1 of the process, all threading lines have been crossed and bent by 90° either to left or to right, depending on their relative position from the middle of the mask opening. Therefore after that time, during step 2, the whole upper volume of the overgrowth comprised between the coalescence boundaries is free of vertically threading defects as observed by TEM observation on plane views.

 © 1999 COSiW SEP, Warsaw

5.7. Luminescence of GaN obtained by epitaxial lateral overgrowth

Figure 10 shows the luminescence spectrum of undoped GaN grown on the top of a pseudo-substrate obtained by the two-step process described above after reactor cleaning to minimise Mg contamination. This kind of spectrum is representative and has been observed with a small variation for different samples grown following the same process. The main feature is the sharpness of the peaks. GaN layers grown directly on sapphire in the same reactor have FWHM of about 3 meV in the best cases. FWHMs below 1 meV are achieved for the bound excitons. This is comparable to the results reported for homoepitaxial GaN [45] and HVPE GaN [46–47]. The free excitons A and B are well resolved as well as the three emission lines labelled A* attributed to excited states of A following [46].

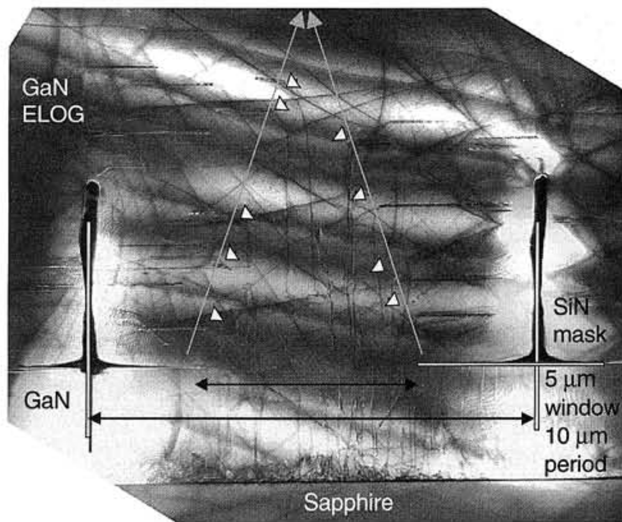

Fig. 9. TEM cross-section view of GaN overgrown with the two-step process.

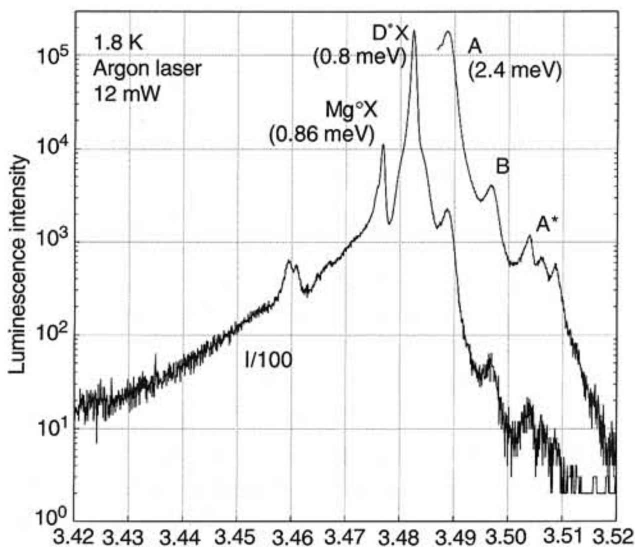

Fig. 10. Low temperature luminescence spectrum measured on undoped GaN grown on the top of a pseudo GaN substrate obtained by the to two-step overgrowth process.

6. Coalescence from islands

6.1. Introduction

Even though ELOG technology has creates a breakthrough in the heteroepitaxy of GaN, a new process using basically the same growth mechanisms has been implemented. We have shown that the introduction of SiH_4 in the early stages of the process significantly improves the quality of the GaN layers. Also, it has been demonstrated that the composition of the carrier gas (H_2 + N_2) is of critical importance for the growth process. Basically, improved nucleation promotes lateral growth from high quality GaN starting islands on sapphire [48–51].

The influence of two adjustable parameters on the resulting film quality, an *in situ* sapphire surface preparation and the carrier gas composition, are thereafter discussed. A three-dimensional (3D) growth mode of the buffer leads to the best materials with a defect density in the mid 10^8 cm^{-2} range which can be compared to the state of art results for MOVPE GaN on sapphire.

6.2. Experimental

Two *in situ* sapphire preparations were investigated. The first *in situ* preparation is the standard nitridation performed at 1050–1080°C during 10 minutes under NH_3. The second preparation consists in the former nitridation followed by an *in situ* deposition of a thin silicon nitride coating on the sapphire substrate. The SiN coating is obtained by introducing silane in the vapour phase at the end of the nitridation step of sapphire. After completion of one of these *in situ* preparations of sapphire, a 25–30 nm thick GaN buffer layer is deposited at 600°C. The epilayers are then grown at 1080°C

Thereafter, two different types of carrier gas were used; either pure N_2 or a mixture of N_2 and H_2 with an appropriate surface treatment (nitridation and silicon nitride coating), conditions for a 3D growth mode of the buffer layer were established. At this stage almost self-organised pyramids are obtained like in a selective epitaxy (Fig. 11). In this nucleation stage, Si plays the role of an "anti-surfactant", promoting 3D growth [52] (whereas Mg leads to 2D mode).

Afterwards, a proper choice of the composition of the vapour phase (H_2+N_2) induces lateral growth similar to the ELOG process. All these different stages of the process can be followed by *in situ* real time LR. Details are given in [48–51].

The process represents a major improvement in the growth of MOVPE. The main characteristics of the 3D growth mode appearing in the improved process are the island formation from the buffer layer and the further coalescence of the GaN islands which allows surface smoothing or other islands shapes. This island appearance is observed when the mixture H_2:N_2 is used as carrier gas. H_2 seems to act as a "morphactant" as Eaglesham et al. [54] called impurities, which favoured particular equilibrium shapes of islands. It has to be noticed that similar 3D growth has already been observed when using pure H_2 as carrier gas [24,51]. In standard samples, the defects present in the volume of the films are **a** dislocations (10^{10} cm^{-2}) and nanopipes (10^{8} cm^{-2}) [53].

6.3. Structural assessment

The **a** dislocations are intergrain dislocations. The high density of dislocations is therefore the results of the columnar microstructure observed at every steps of the growth including the buffer layer. In the present process, the reduction of defects mainly affects **a** dislocations. The **a** dislocations, which are not present in the growth islands, appear when the islands coalesce and become also intergrain dislocations. But their density is considerably reduced due to the larger lateral size of the islands when compared to that of the columns in standard samples.

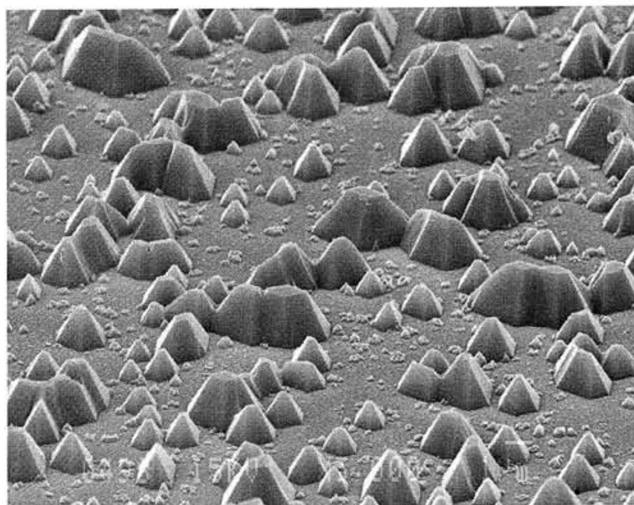

Fig. 11. SEM photographs of the NL, heated up to 1050°C after nitridation of the sapphire and SiH_4 treatment.

The morphology of the sample shown in Fig. 11 is very similar, though at a lower scale, to that observed in the selective area epitaxy (SAE) as described first by Hiramatsu et al. [55]: islands with well defined truncated pyramidal with the (0001) top surface and {10–11} lateral facets. In SAE, the micrometer large islands are separated by bare SiO_2 selective masks whereas in the process described here, the hundred nanometers large islands are separated by SiN coated bare sapphire surface which also presents non nucleation behaviour. In many aspects, the growth of GaN on *in situ* SiN coated sapphire presents a strong analogy with SAE except for the dimension scale and for the fact that openings in the mask are induced by the *in situ* SiN partial coverage. The coalescence and smoothing phenomena, which lead to specular films, implies that the growth rate of islands is significantly anisotropic.

The adatoms resulting from decomposition of the precursors diffuse on the bare surface, owing to the apparent large surface mobility of SiN coated sapphire, meet pre-existent islands and therefore participate to the lateral growth.

The comparison of 3D growth and classical 2D growth on GaN buffer layer is shown in Fig. 12. For sample (a) (3D), only threading dislocations were visible. For the classical 2D layer, a few pipes were presented. Images (a) and (b) show a representative surface of 1.5 μm^2 for each sample. On image (a), only 7 threading dislocations emerge where 200 are counted for the classical sample. This leads to a defect density of 4×10^{8} cm^{-2} against 10^{10} cm^{-2} [56].

7. Conclusions

Presently, nitride based LSD and LEDs have been fabricated by MOVPE. Despite great complexities, MOVPE can produce GaN from trimethyl gallium and ammonia with qualities relevant for electronic and optoelectronic devices. Since GaN growth on non-lattice matched substrates like sapphire or 6H-SiC, a huge density of defects results that, to some extend, does not limit too much the lifetime of devices. However, reduced defects densities GaN have proven to produce better devices.

Henceforth, the large densities of dislocations can be significantly reduced (by about three orders of magnitude) using appropriate lateral growth technologies. This, therefore, allows producing LDs with 10,000 hours lifetime. A simpler process using basically the same growth mode led to GaN sample with about 10^{8} cm^{-2} dislocations, which represents a sub-

 © 1999 COSiW SEP, Warsaw

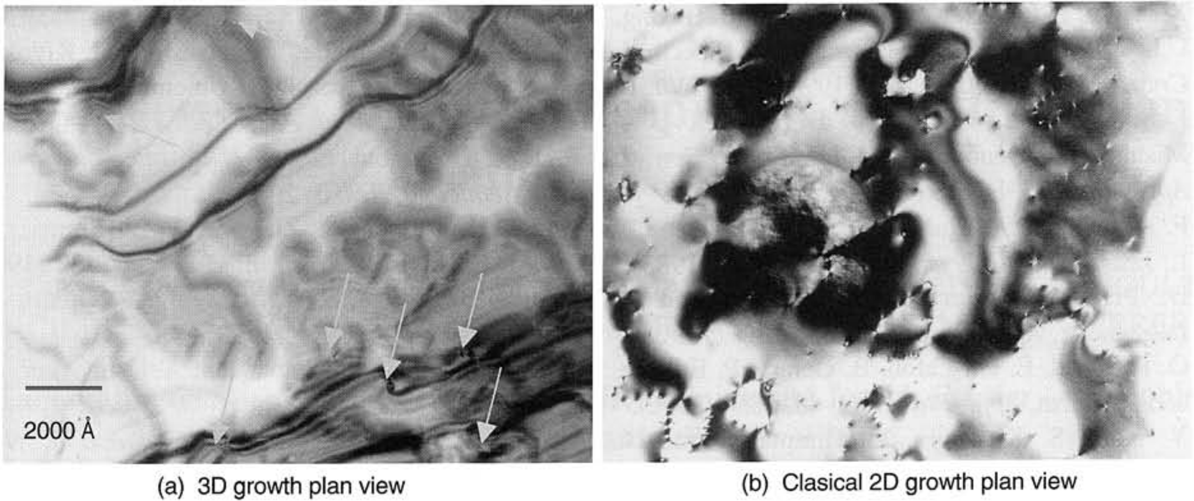

Fig. 12. Plan view images of GaN layers: (a) 3D growth and coalescence of islands, (b) standard three-step process.

stantial improvement compared to the three-step method, without any of technological steps of the ELOG technology. Mechanisms of propagation of dislocations have also been evaluated. Also the electronic behaviour of extended defects need to be fully assessed.

Acknowledgements

The authors would like to thank Dr. S. Haffouz, M. Passerel, Dr. M. Leroux, M. Teisseire, M. Vaille, and Dr. G. Neu for their helpful contribution to this work. Special thanks are also expressed to T. Boufaden for the use of Fig. 1 and 3, and H. Larèche for Fig. 11 and 12 prior to publication. All HRTEM data reported in the present paper were produced by P. Vennegués and his invaluable contribution is greatly appreciated. This work is supported by EU contracts ESPRIT

References

1. R. Dingle, R. Shaklee, R.F. Leheny, and R.B. Zetterstrom, *Appl. Phys. Lett.* **19**, 5 (1971).
2. H. Amano, I. Akasaki, T. Kozawa, K. Hiramatsu, N. Sawaki, K. Ikeda, and Y. Ishii, *J. Lumin.* **40-48**, 121 (1988).
3. H. Amano, M. Kito, K. Hiramatsu, and I. Akasaki, *Jpn. J. Appl. Phys.* **28**, L2112 (1989).
4. S. Nakamura, T. Mukai, M. Senoh, and N. Iwasa, *Jpn. J. Appl. Phys.* **31**, 1258 (1992).
5. S. Nakamura and G. Pajol, *The Blue Laser Diode*, Berlin, Springer, 1997.
6. S. Nakamura et al., *J. Cryst. Growth* **189/190**, 820 (1998).
7. B. Beaumont, M. Vaille, T. Boufaden, B. el Jani and P. Gibart, *J. Cryst. Growth* **170**, 316 (1997).
8. B. Beaumont, P. Gibart, and J.P. Faurie, *J. Cryst. Growth* **156**, 140 (1995) and references therein; B. Beaumont and P. Gibart, *Proc. Intern. Conf. on Semiconductor Heteroepitaxy (ICSH'95)*, edited B. Gil and R.L. Aulombard, World Scientific p. 258 (1995).
9. The «GEMINI» code was provided by «THERMODATA», Grenoble (France)
10. M. Sato, *Solid-State Electronics* **41**, 223 (1997).
11. B. Zhou, X. Li, T.L. Tansley, and K.S.A. Butcher, *J. Cryst. Growth* **160**, 201 (1996).
12. B. Zhou, X. Li, T.L. Tansley, K.S.A. Butcher, H. Zou, and T.L. Tansley, *Solid State Electron.* **41**, 279 (1997).
13. H. Sato, H. Takahashi, and A. Watanabe, *Appl. Phys. Lett.* **68**, 3617 (1996).
14. A. Freedman and G.N. Robinson, *Mater. Res. Soc.* **73** (1996).
15. D.G. Chtchekine el al., *J. Appl. Phys.* **81**, 2197 (1997).
16. C.R. Jones, T. Lei, R. Kaspi, and K.R. Evans, *Mater. Soc. Res.* **141**, 5 (1996).
17. N. Newman, *J. Cryst. Growth* **178**, 102 (1997).
18. D.A. Neumayer et al., *Mater. Res. Soc.* **85**, (1966).
19. K. Uchida et al., *J. Appl. Phys.***79**, 3487 (1996).
20. Ph. Vennegués, private communication.
21. S. Keller et al., *Appl. Phys. Lett.* **68**, 1525 (1996).
22. W. Van der Stricht et al., *J. Cryst. Growth* **170**, 344 (1997).
23. X.H. Wu et al., *J. Appl. Phys.* **80**, 3228 (1996).

24. X.H. Wu, P. Fini, S. Keller, E.J. Tarsa, B. Heying, U.K. Mishra, S.P. Denbaars, and J.S. Speck, *J. Cryst. Growth* **189/190**, 231 (1998); X.H. Wu, P. Fini, S. Keller, E.J. Tarsa, B. Heying, U.K. Mishra, S.P. Denbaars, and J.S. Speck, *Jpn. J. Appl. Phys.* **35**, L1648 (1996).
25. F. A. Ponce, *MRS Bull.* **22**, 51 (1997).
26. L. Jastrzebski, *J. Cryst. Growth* **63**, 493 (1983).
27. D. Pribat, B. Gerard, M. Dupuy, and P. Legagneux, *Appl. Phys. Lett.* **60**, 2144 (1992).
28. O. Parillaud, E. Gil-Lafon, B. Gérard, P. Etienne, and D. Pribat, *Appl. Phys. Lett.* **68**, 2654 (1996).
29. Y. Kato, S. Kitamura, K. Hiramatsu, and N. Sawaki, *J. Cryst. Growth* **144**, 133 (1994).
30. S. Kitamura, K. Hiramatsu, and N. Sawaki, *Jpn. J. Appl. Phys.* **24**, L1184 (1995).
31. T. Detchprohm, T. Kuroda, K. Hiramatsu, N. Sawaki, H. Goto, *Inst. Phys. Conf. Ser.* **142**, 859,1996
32. D. Kapolnek, S. Keller, R. Vetury, R.D. Underwood, P. Kozodoy, S.P. DenBaars, and U.K. Mishra, *Appl. Phys. Lett.* **71**, 1204 (1997).
33. O.H. Nam, M.D. Bremser, and T.S. Zheleva, R.F. Davis, *Appl. Phys. Lett.* **71**, 2638 (1997).
34. T.S. Zheleva, O.H. Nam, M.D. Bremser, and R.F. Davis, *Appl. Phys. Lett.* **71**, 2472 (1997).
35. O. Nam, M.D. Bremser, B.L. Ward, R.J. Nemanich, and R.F. Davis, *Jpn. J. Appl. Phys.* **36**, L532 (1997).
36. A. Usui, H. Sunakawa, A. Sakai, and A.A. Yamaguchi, *Jpn. J. Appl. Phys.* **36**, L899 (1997).
37. H. Marchand, J.P. Ibbetson, P.T. Fini, P. Kozodoy, S. Keller, S. DenBaars, J.S. Speck, and U.K. Mishra, *MRS Internet J. Nitride Semicond. Res.* **3**, 3 (1998).
38. Z. Yu, M.A.L. Johnson, T. Mcnulty, J.D. Brown, J.W. Cook, and J.F Schetzina, *MRS Internet J. Nitride Semicond. Res.* **3**, 6 (1998).
39. B. Beaumont, P. Gibart, M. Vaille, S. Haffouz, G. Nataf, and A. Bouillé, *J. Cryst. Growth* **189/190**, 97 (1998).
40. S. Nakamura, M. Senoh, S. Nagahama, N. Iwasa, T. Yamada, T. Matsushita, H. Kiyoku, Y. Sugimoto, T. Kozaki, H Umemoto, M. Sano, and K. Chocho, *Appl. Phys. Lett.* **72**, 211 (1998).
41. B. Beaumont et al., *MRS Internet J. Nitride Semicond. Res.* **3**, 20 (1998).
42. O.H. Nam, T.S. Zheleva, M.D. Bremser, and R.F. Davis, *J. Electron. Mater.* **27**, 233 (1998).
43. B. Beaumont, S. Haffouz, and P. Gibart, *Appl. Phys. Lett.* **72**, 921 (1998).
44. A Sakai, H. Sunakawa, and A. Usui, *Appl. Phys. Lett.* **71**, 2259 (1997).
45. H. Teisseyre et al., *MRS Internet J. Nitride Semicond. Res.* **1**, 13 (1996).
46. A. Hoffmann and L. Eckey, *Materials Science Forum* **264/268**, 1259 (1998).
47. M. Leroux, B. Beaumont, N. Grandjean, P. Lorenzini, S. Haffouz, P. Vennegues, J. Massies, and P. Gibart, *Mater. Sci. Eng.* B **50**, 97 (1997).
48. S. Haffouz et al., *Appl. Phys. Lett.* **73**, 1278 (1998).
49. P. Vennegues, B. Beaumont, S. Haffouz, M. Vaille, and P. Gibart, *J. Cryst. Growth* **187**, 167 (1998).
50. S. Haffouz, B. Beaumont, and P. Gibart, *MRS Internet J. Nitride Semicond. Res.* **3**, 8 (1998).
51. J. Han, T.B. Ng, R.M. Biefield, M.H. Crawford, and D.M. Follstaedt, *Appl. Phys. Lett.* **71**, 3114 (1997)
52. X.Q. Chen, S. Tanaka, S. Iwai, and Y. Aoyagi, *Appl. Phys. Lett.* **72**, 344 (1998).
53. P. Vennegues, B. Beaumont, M. Vaille, and P. Gibart, *J. Cryst. Growth* **173**, 249 (1997).
54. D.J. Eaglesham, F.C. Unterwald, and D.C. Jacobson, *Phys. Rev. Lett.* **70**, 966 (1993).
55. K. Hiramatsu, S. Kitamura, and N. Sawaki, *Mater. Res. Symp. Proc.* **395**, 267 (1996).
56. H. Larèche, unpublished.

 © 1999 COSiW SEP, Warsaw